Letter

ADVANCED PHOTONICS

Two-channel, dual-beam-mode, wavelength-tunable femtosecond optical parametric oscillator

Jintao Fan,[a] Jun Zhao,[a] Liping Shi,[b,c] Na Xiao,[a] and Minglie Hu[a,*]

[a]Tianjin University, College of Precision Instrument and Optoelectronics Engineering, Ultrafast Laser Laboratory, Tianjin, China
[b]Leibniz Universität Hannover, Institut für Quantenoptik, Hannover, Germany
[c]Cluster of Excellence PhoenixD (Photonics, Optics, and Engineering-Innovation Across Disciplines), Hannover, Germany

Abstract. Optical vortices, which carry orbital angular momentum, offer special capabilities in a host of applications. A single-laser source with dual-beam-mode output may open up new research fields of nonlinear optics and quantum optics. We demonstrate a dual-channel scheme to generate femtosecond, dual-wavelength, and dual-beam-mode tunable signals in the near infrared wavelength range. Dual-wavelength operation is derived by stimulating two adjacent periods of a periodically poled lithium niobate crystal. Pumped by an Yb-doped fiber laser with a Gaussian ($l_p = 0$) beam, two tunable signal emissions with different beam modes are observed simultaneously. Although one of the emissions can be tuned from 1520 to 1613 nm with the Gaussian ($l_s = 0$) beam, the other is capable of producing a vortex spatial profile with different vortex orders ($l_s = 0$ to 2) tunable from 1490 to 1549 nm. The proposed system provides unprecedented freedom and will be an exciting platform for super-resolution imaging, nonlinear optics, multidimensional quantum entanglement, etc.

Keywords: nonlinear optics; parametric processes; optical parametric oscillators; ultrafast nonlinear optics.

Received Feb. 29, 2020; revised manuscript received Jun. 5, 2020; accepted for publication Jun. 22, 2020; published online Jul. 6, 2020.

[DOI: 10.1117/1.AP.2.4.045001]

Optical vortex beams, carrying orbital angular momentum (OAM), have a helical phase front and exhibit a doughnut intensity distribution. The unique phase distribution can be described by an azimuthal phase dependence $\exp(il\alpha)$, where l being an integer is known as the topological charge of the beam and α is the azimuthal angle.[1,2] Since the first demonstration, optical vortices have garnered tremendous interest and have been applied in various fields such as quantum optics, microscopy, and optical communication.[3–5] Spurred by these applications, approaches to generating OAM-carrying beams have become a current subject of intense research. Basically, the methods for generating the optical vortices can be classified into passive and active categories, depending on whether the vortices are created directly at the source. The direct emission from a laser cavity, namely the active method, has raised great interest due to its excellent features of compactness, high efficiency, and high purity.[6] Furthermore, dual-beam-mode (one Gaussian beam and one OAM beam) illumination sources have been shown to be suitable for extreme ultraviolet self-torqued beams, high harmonic generation, and super-resolution imaging.[7–9] On the other hand, to fulfill the requirement of the applications in super-resolution imaging, pump-probe spectroscopy, and tunable terahertz generation, the OAM laser source, which can provide multiple output wavelengths with an independent tuning range, is highly demanded. Despite fruitful efforts having been made to generate optical vortices, to the best of our knowledge, no technique has been reported to deliver wavelength-tunable dual-beam modes directly at the source.

Optical parametric oscillators (OPOs) have shown to be compelling alternatives for generating vortex beams by proving the combination of high output power, broad wavelength coverage, and tunable vortex orders.[10–14] Previous efforts have focused on the transfer of the OAM in OPOs from the pump to the output beams. The OAM of the pump vortex beam can be selectively transferred to one of the generated waves (signal or idler beam) by controlling the cavity losses.[10] Nevertheless, owing to the vortex nature of the pump beam and hence the lower nonlinear gain (compared to the Gaussian pump), the output power is

*Address all correspondence to Minglie Hu, E-mail: huminglie@tju.edu.cn

limited. In addition, the controlling OAM modes in such schemes at a higher order vortex pump are significant challenges to overcome. On the other hand, dual-wavelength OPOs have been proposed to produce two tunable radiation pairs simultaneously.[15–19] For instance, using two different nonlinear crystals in a single OPO, while adjusting the grating periods of the crystals, Jin et al.[17] generated tunable dual-wavelength output pulses in the mid-infrared region. However, this cavity structure requires two nonlinear crystals, which makes the system more expensive. In 2014, Gu et al.[18] reported a tunable dual-wavelength femtosecond visible OPO, achieved by introducing a prism pair inside the OPO cavity. Such a configuration ensures independent tuning of two central wavelengths conveniently, which will benefit many applications.

In this work, we combine these two technologies by developing for the first time a two-channel, dual-pumped OPO configuration that is capable of providing dual-wavelength, dual-beam modes tunable across the telecommunication band. Two pump beams are incident onto two adjacent poling periods of a single periodically poled lithium niobate (PPLN) crystal. Such a structure ensures that two independently tunable pairs of signals can achieve synchronism with the pump and oscillate simultaneously, by adjusting the OPO cavity length of each channel. In this way, the OPO generates two signals tunable over 1520 to 1613 nm and 1490 to 1549 nm, respectively. We also show that the vortex beams with different OAM modes are created in one channel of our system, while keeping the other channel in Gaussian beam mode. The proposed method opens a new window to generating dual-beam-mode lights with a simple cavity design, which may lead to advances in a wide range of applications in microscopy and quantum optics.

The experimental setup for the proposed OPO is schematically illustrated in Fig. 1. It starts from a homemade Yb-doped fiber laser amplifier system, which has the following parameters: repetition rate of 53 MHz, central wavelength of 1040 nm, pulse duration of 80 fs, and maximum average output power of 4 W. The Gaussian distributed pump beam is split equally into two orthogonal directions using the combination of a half-wave plate (HWP1) and a polarization beam splitter (PBS). HWP2 is employed here to further adjust the polarization state of the pump beam to be horizontal, thus fulfilling the phase-matching condition of the OPO crystal. Two separated beams are focused into the adjacent period of the nonlinear crystal by convex lenses L1 and L2, respectively. A single 1-mm-long multigrating MgO-doped PPLN (MgO:PPLN), which contains seven gratings with periods ranging from 28.5 to 31.5 μm in steps of 0.5 μm, is used for OPO operation. The crystal is antireflectively coated over 1300 to 1900 nm ($R < 2\%$) and 2200 to 4800 nm ($R < 10\%$) and exhibits a reflective coefficient lower than 1% at around 1040 nm.

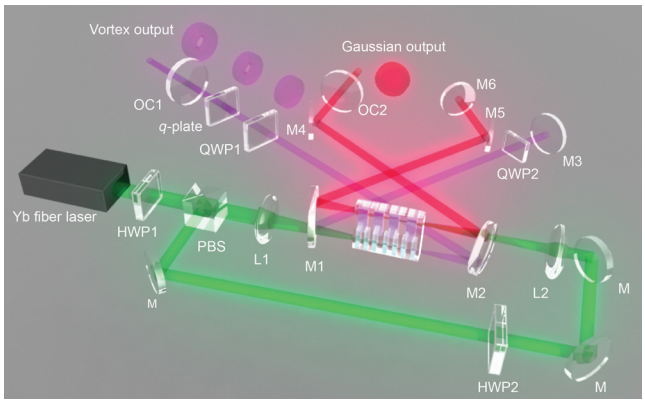

Fig. 1 Schematic illustration of the experimental set-up. L1 and L2: lenses; HWP: half-wave plate; PBS: polarization beam splitter; QWP: quarter-wave plate; M1 to M4: dielectric mirrors; and OC: 15% output coupler. The red and purple beams present the signal for channel 1 and channel 2, respectively.

The OPO cavity configuration can be divided into two channels: the upper channel (channel 1) for generating Gaussian beams and the lower channel (channel 2) for producing vortex beams. Both channels are configured in a standing-wave cavity with an X-type folding. The two channels share the nonlinear crystal and concave mirrors (M1 and M2); however, the injection poling periods of the PPLN for channel 1 and channel 2 are set to be 30.5 and 30 μm, respectively. The Gaussian beam oscillates in the cavity composed of mirrors M1, M2, M4–M6, and output coupler 2 (OC2) (channel 1), while channel 2 includes mirrors M1, M2, M5, and OC1. A pair of quarter-wave plates (QWPs) and a q plate with $q = 1/2$ are introduced into this channel to generate vortex signals. All mirrors are highly reflective ($R > 99\%$) for the signals over 1350 to 1650 nm and highly transmitting ($T > 90\%$) for the idler and pump, resulting in the single-resonant signal oscillation. OC1 and OC2 are mounted on a delay line to provide the required adjustment of the cavity length of the two channels. Therefore, the total optical length of each channel is ~2.83 m, thus ensuring synchronization to the pump laser repetition rate. Furthermore, by changing cavity length, wavelength tuning can be separately achieved for each channel.

In theory, the beam profile and polarization state of the signal should be preserved after each round trip in an OPO cavity. The mode reversibility in channel 1 is easily realized. Here we mainly focus on channel 2, where a pair of QWPs and a q-plate are inserted into the cavity. Figure 2(a) depicts the evolution of the signals in a round trip when a q-plate of $q = 1/2$ is employed. The q-plate can be seen as an inhomogeneous birefringent element.[6] The right circularly polarized Gaussian beam is converted into a vortex beam with left circular polarization. On the other hand, in terms of intrinsic conversion nature of the Gaussian beam pumped OPO, only the phase matched signal can be amplified. That is to say, only horizontally polarized Gaussian signals can obtain parametric gain in the proposed system. For these two reasons, the inclusion of QWP1 and QWP2 with the optics axis rotated 45 deg with respect to the horizontal axis is utilized inside the OPO cavity. Based on this arrangement, the polarization state of the signal inside the OPO cavity is precisely controlled to fulfill both the parametric down conversion and mode conversion conditions. As can be seen in Fig. 2(a), the pump and signal both are polarized horizontally to achieve the highest conversion efficiency of PPLN (in the direction of the pump). The vortex signal output can also be obtained when the horizontally polarized signal passes through QWP1 and the q-plate. Furthermore, such a scheme also ensures that the beam mode and polarization state are reproduced after each round trip. As shown in Fig. 2(b), the reversible light transformation process is derived using Jones matrices.[20]

To characterize the proposed dual-channel OPO, we initially performed wavelength measurement by tuning the cavity length of each channel individually, as commonly used in femtosecond laser pumped OPOs.[21] It should be noted that coherent coupling

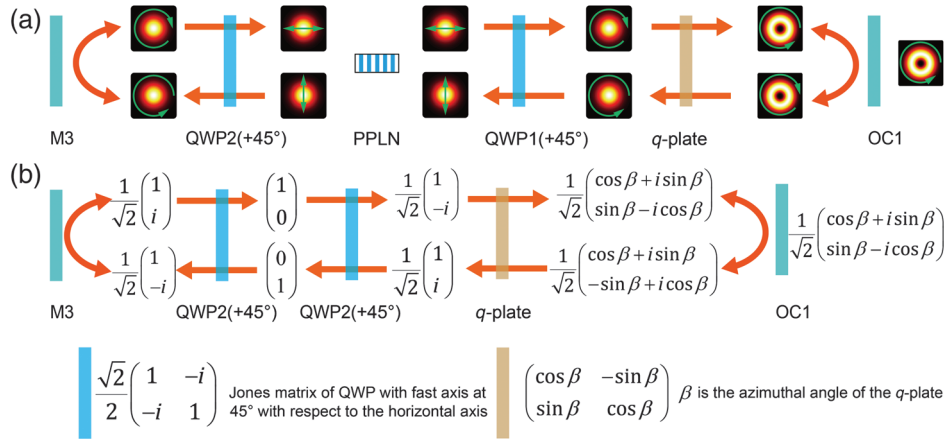

Fig. 2 Working principle. (a) The evolution of signal beam profiles and polarization states through one round trip in the lower channel of OPO. Green arrows correspond to the polarization of light. (b) Jones matrices of basic optical elements and propagation beams.

between two signals is completely avoided as a result of the cavity design. The two signals operate separately and as such can be varied independently and uninterruptedly across the OPO tuning range. The dual-channel OPO wavelength tuning behavior is shown in Fig. 3(a) when the pump power is fixed to be 2 W for each channel. By changing the cavity length of channel 1, the central wavelength of the signal can be continuously tuned from 1521 to 1613 nm. For channel 2, a spectral shift from 1490 to 1549 nm is obtained when the cavity length is varied. Different combinations of cavity length lead to spectra with different central frequency separations. As evident from Fig. 3(a), central wavelength differences ranging from 0.51 to 15.21 THz are realized. Notably, the central wavelength difference can be further reduced to 0 (degenerate point) when two spectra overlap. In this way, two identical signals with different beam modes are obtained, without affecting one another. Furthermore, the degenerate point can be shifted arbitrarily within the overlapping spectral range of two signals.

We further recorded the spatial intensity profile of signal beams for both channels, with the results shown in Fig. 3(b). As expected, the signal from channel 1 possesses Gaussian intensity distribution ($l_s = 0$), whereas for channel 2, due to the insertion of QWPs and the q-plate, the signal beams have doughnut intensity profiles when the angles of QWPs are set to be $+45$ deg and -45 deg, respectively. To confirm the vortex order of the generated signal, we characterize the signal beams using the tilted lens technique[22] in which a vortex beam of order $|l|$ will split into $|l|+1$ lobe after passing through a tilted lens. The lobe structures show that the signal beams have a vortex order of $+1$ and -1. The sign of the vortex beams, which indicates the direction of phase variation, is evident from the orientation of the bright spots. To further confirm the absence of the phase singularity, we performed interference experiments by self-interfering the signals using a Mach–Zehnder interferometer. The recorded fork interference patterns are also depicted in Fig. 3(b), and it is evident that both beams carry OAM, which is the hallmark of the optical vortex. In addition, it should be pointed out that the signal retains the same properties (the average output power, pulse duration, and optical spectrum) except for the phase singularity when the orientation of the QWPs is switched.

After confirming the successful generation of dual-beam-mode signals in different channels, we measured the output power and pulse duration across the tuning range, as displayed in Fig. 4. As is evident from Fig. 4(a), for a constant pump power of 2 W, the Gaussian signal power from channel 1 varies

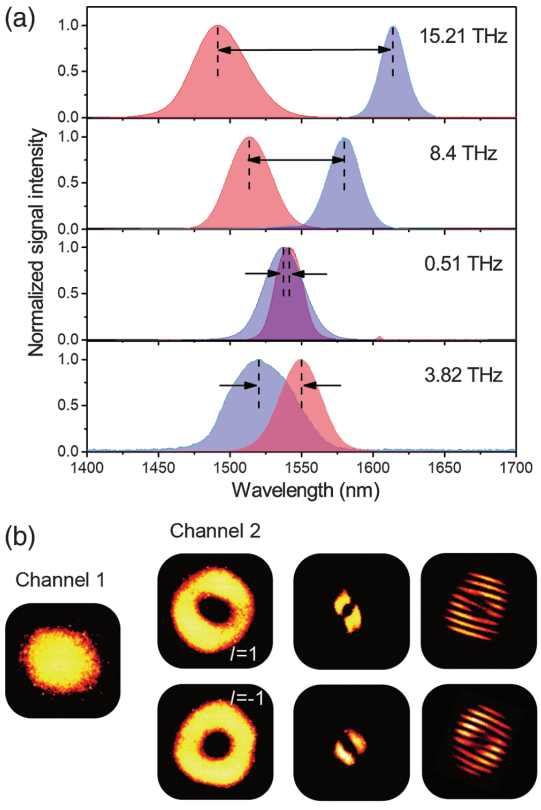

Fig. 3 Spectral properties and beam profiles of the output. (a) Measured signal spectra (blue area and red area are for channel 1 and channel 2, respectively) by tuning cavity length of each channel. (b) Output intensity profiles for both channels. Corresponding lobe structure and interference pattern of the vortex beams are also shown here.

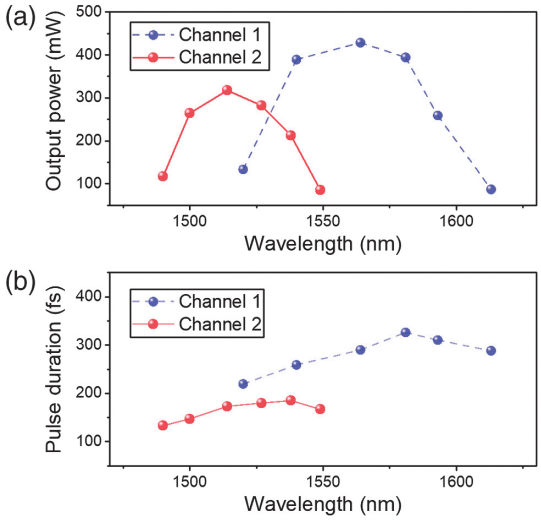

Fig. 4 Output power of the proposed OPO. (a), (b) Variations of the (a) signal output power and (b) pulse durations versus the central wavelength in different channels.

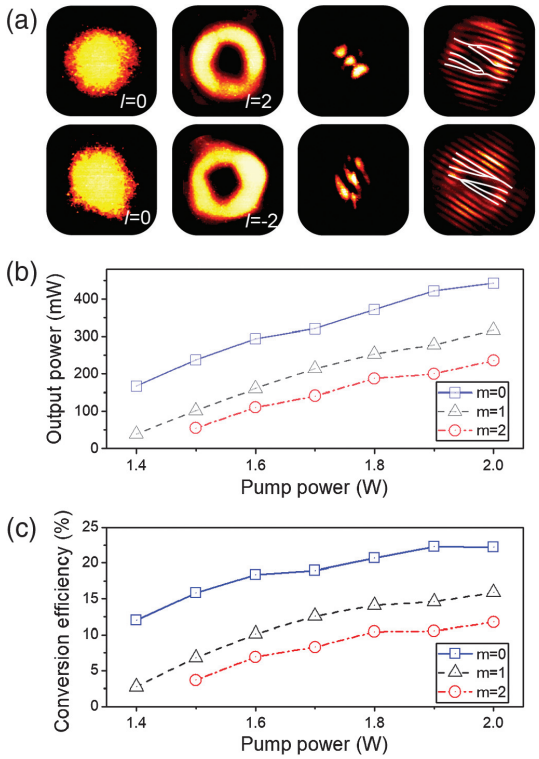

Fig. 5 (a) Far-field intensity distribution of the Gaussian signal beams and vortex signal beams of vortex order $l_s = \pm 2$ from channel 2. Tilted lens image and self-referencing of the vortex signal beams are also shown here. (b), (c) Variation of the signal output power and pump-signal conversion efficiency with the pump power for different vortex orders in channel 2.

from 133 mW at 1520 nm, to 87 mW at 1613 nm, with a maximum output power of 428 mW at 1564 nm. For vortex signal output from channel 2, the output power is 117 mW at a central wavelength of 1490 nm and 85 mW at 1549 nm. The maximum signal output power is 317 mW at 1514 nm. The decrease of the vortex signal output power of channel 2, as compared with the Gaussian signal output of channel 1, can be attributed to both the mode conversion loss of the q-plate and the extra introduction loss of QWPs. Figure 4(b) shows the pulse duration of the signal. With a Gaussian pulse shape assumption, the pulse durations for channel 1 and channel 2 are around 282 and 165 fs, respectively. Obviously, the pulse durations of Gaussian signals from channel 1 are longer than those of vortex signals from channel 2, which can be ascribed to the different group delay dispersions introduced by the intracavity optical elements (PPLN, QWPs, q-plate, and mirrors).

Moreover, the scheme of channel 2 can be used to generate different order vortex beams by simply changing the topology charge of the q-plate. In the following experiment, we operate the OPO in channel 2 at a signal wavelength of 1514 nm, where maximum output power is obtained. By simply moving the q-plate of $q = 1/2$ out of the cavity or replacing it with a q-plate of $q = 1$, we obtained Gaussian signal beams (vortex order of $l_s = 0$) and vortex signal beams of vortex order $|l_s| = 2$; the far-field intensity beam profiles are presented in the first and second columns of Fig. 5(a). Both the corresponding lobe structure and interference pattern confirm the vortex order of the signal. By adjusting the angle of QWPs, signal beams carrying a vortex order with opposite signs can be easily achieved [see the second row of Fig. 5(a)].

We also investigated the influence of the insertion of a q-plate on the signal output power. For that, we compared variation of the average output power with the pump power in different cases (see Fig. 5). With a fixed pump power of 2 W, we measured a maximum signal output power of 445 mW (317 and 235 mW) for the signal vortex of the order $l_s = 0$ ($l_s = 1$ and $l_s = 2$). Figure 5(c) compares the conversion efficiency of the signal on the vortex order of $l_s = 0$, $l_s = 1$, and $l_s = 2$. The maximal conversion efficiencies for the $l_s = 0$, $l_s = 1$, and $l_s = 2$ vortices are 22.2%, 15.9%, and 11.8%, respectively. The difference in output power and conversion efficiency can be attributed to the transmission loss and mode conversion loss introduced by the q-plate. Indeed, the transmittance of the q-plate for the whole wavelength tuning range is over 98%; thus the transmission loss can be negligible. It is well known that the vortex beam possesses a spiral phase front about a singularity point where the phase is undefined, leading to a central null in beam profile.[23] This central hole is responsible for the losses in output power for different orders. The loss caused by this phase singularity point is termed as mode conversion loss. Essentially, the central null of the annular beam becomes larger as the order of the q-plate increases, and accordingly the mode conversion loss increases with the increase of the vortex beam order.

In conclusion, with the purpose of delivering dual-wavelength, dual-beam-mode signals with independent tuning, we designed a new dual-channel scheme in a femtosecond OPO. By introducing a pair of QWPs and a q-plate in one channel, the OPO delivers signals tunable from 1520 to 1613 nm with the Gaussian beam profile and from 1490 to 1549 nm with the vortex beam profile, respectively. Furthermore, our results also provide an alternative for generating different order vortex beams by simple adjustment of the q-plate with the proper vortex order. Given that q-plates are placed in both channels, dual-OAM-beam-mode output can be readily obtained. Our scheme enables dual-color operation with different beam profiles, thus representing

a promising solution for efficient generation of tunable THz radiation, optical microscopy, super resolution imaging, etc.

Acknowledgments

We gratefully acknowledge the financial support by the National Natural Science Foundation of China (NSFC) (Nos. 61535009 and 6182781) and the Tianjin Research Program of Application Foundation and Advanced Technology (No. 17JCJQJC43500). There are no conflicts of interest in this work.

References

1. M. Yao et al., "Orbital angular momentum: origins behavior and applications," *Adv. Opt. Photonics* **3**, 161–204 (2011).
2. Y. Shen et al., "Optical vortices 30 years on: OAM manipulation from topological charge to multiple singularities," *Light Sci. Appl.* **8**(1), 90 (2019).
3. A. Mair et al., "Entanglement of the angular momentum states of photons," *Nature* **412**, 313–316 (2001).
4. A. E. Willner et al., "Optical communications using orbital angular momentum beams," *Adv. Opt. Photonics* **7**, 66–106 (2015).
5. S. Bernet et al., "Quantitative imaging of complex samples by spiral phase contrast microscopy," *Opt. Express* **14**(9), 3792–3805 (2006).
6. D. Naidoo et al., "Controlled generation of higher-order Poincaré sphere beams from a laser," *Nat. Photonics* **10**, 327–332 (2016).
7. L. Rego et al., "Generation of extreme-ultraviolet beams with time-varying orbital angular momentum," *Science* **364**, eaaw9486 (2019).
8. F. Kong et al., "Tunable orbital angular momentum in high-harmonic generation," *Nat. Commun.* **8**, 14970 (2017).
9. G. Vicidomini et al., "STED super-resolved microscopy," *Nat. Methods* **15**, 173–182 (2018).
10. A. Aadhi et al., "Controlled switching of orbital angular momentum in an optical parametric oscillator," *Optica* **4**, 349–355 (2017).
11. A. Aadhi et al., "Continuous-wave, singly resonant parametric oscillator-based mid-infrared optical vortex source," *Opt. Lett.* **42**, 3674–3677 (2017).
12. V. Sharma et al., "Orbital angular momentum exchange in a picosecond optical parametric oscillator," *Opt. Lett.* **43**, 3606–3609 (2018).
13. V. Sharma et al., "Tunable ultraviolet vortex source based on a continuous-wave optical parametric oscillator," *Opt. Lett.* **44**, 4694–4697 (2019).
14. V. Sharma et al., "Controlled generation of vortex and vortex dipole from a Gaussian pumped optical parametric oscillator," *Opt. Express* **27**(13), 18123–18130 (2019).
15. F. Ganikhanov et al., "Broadly tunable dual-wavelength light source for coherent anti-Stokes Raman scattering microscopy," *Opt. Lett.* **31**, 1292–1294 (2006).
16. A. Esteban-Martin et al., "Dual-wavelength optical parametric oscillator using antiresonant ring interferometer," *Laser Photonics Rev.* **6**, L7 (2012).
17. Y. Jin et al., "Broadly, independent-tunable, dual-wavelength mid-infrared ultrafast optical parametric oscillator," *Opt. Express* **23**(16), 20418–20427 (2015).
18. C. Gu et al., "High-power, dual-wavelength femtosecond LiB_3O_5 optical parametric oscillator pumped by fiber laser," *Opt. Lett.* **39**, 3896–3899 (2014).
19. P. Liu et al., "Dual-channel operation in a synchronously pumped optical parametric oscillator for the generation of broadband mid-infrared coherent light sources," *Opt. Lett.* **43**, 2217–2220 (2018).
20. Y. Zhang et al., "Flexible generation of femtosecond cylindrical vector beams," *Chin. Opt. Lett.* **15**(3), 030007 (2017).
21. T. Lang et al., "High power ultra-widely tuneable femtosecond pulses from a non-collinear optical parametric oscillator (NOPO)," *Opt. Express* **20**(2), 912–917 (2012).
22. P. Vaity et al., "Measuring the topological charge of an optical vortex by using a tilted convex lens," *Phys. Lett. A* **377**, 1154–1156 (2013).
23. Q. Zhang, "Properties of circularly polarized vortex beams," *Opt. Lett.* **31**, 867–869 (2006).

Jintao Fan received his BS degree in electronic science and technology and his PhD in optical engineering from Tianjin University, Tianjin, China, in 2013 and 2019, respectively. He is now working as a research assistant at Leibnitz University Hannover. His research interests include few cycle pulse laser source and structured beam generation.

Jun Zhao received her BS degree in applied physics from the College of Sciences, Northeastern University, Shenyang, China, in 2015. Currently, she is working toward the PhD in optical engineering at Tianjin University. Her main research interests focus on the nonlinear optics and interaction between femtosecond laser and matter.

Liping Shi received his BEng and PhD degrees in 2009 and 2014, respectively. After a postdoc at Leibniz University Hannover, he joined Westlake University as an associate research fellow in January 2020. His research interests focus on ultrafast strong-field nano-optics and nonlinear nanophotonics.

Na Xiao received her BS degree in optoelectronic technology science (in cooperation with Nankai University) from Tianjin University, Tianjin, China, in 2016, where she is currently working toward the PhD in optical engineering. Her research interests include the nonlinear optics and beam shaping.

Minglie Hu received his BS degree in optoelectronics and his PhD in optical engineering from Tianjin University, Tianjin, China, in 2000 and 2005, respectively. He is now a full professor at the School of Precision Instrument and Optoelectronics Engineering, Tianjin University. He is the author of more than 200 peer-reviewed articles. His current research interests include mode-locking laser oscillators and amplifiers, fiber lasers, linear and nonlinear propagation in photonic crystal fibers, and microstructure optical devices.